

# CHEST X-RAY BASED DISEASE ANALYSIS USING CNN

Talatam Aadi Narayana Murthy<sup>1</sup>, Somabathina Aravind<sup>2</sup>, Ravuri Anil Kumar<sup>3</sup>, Shaik Mohammed Khalid<sup>4</sup>

<sup>1-4</sup> UG Students, Dept of Electronics and Communication Engineering, Vasireddy Venkatadri Institute of Technology, Nambur, Andhra Pradesh, India

## ABSTRACT

The paper is centered around advancing medical diagnostics through the utilization of chest X-ray scans for the detection of respiratory and cardiac conditions. The primary focus is on developing and implementing a machine learning-based system for automated disease detection in chest X-ray images. The principal objective of this paper is to develop a resilient and precise system that can autonomously detect and categorize anomalies, specifically pneumonia, in chest X-ray scans. This is obtained and accomplished through the application of machine learning algorithms, including sophisticated techniques like Convolutional Neural Networks (CNNs). These algorithms analyze radiological images to recognize and categorize pathological conditions, contributing to more efficient and precise medical diagnostics. Key components of the paper include data collection, model development, and performance evaluation. In the data collection phase, a diverse dataset of chest X-ray images is compiled, ensuring comprehensive coverage of labeled disease conditions to encompass a wide spectrum of cases. The model development phase explores various machine learning architectures to construct an accurate disease detection model, with an emphasis on leveraging CNNs for their efficacy in image analysis. Performance evaluation is conducted using standard medical imaging metrics, including sensitivity, specificity, accuracy, and the area under the receiver operating characteristic curve (AUC-ROC). These metrics provide a comprehensive assessment of the system's ability to correctly identify and classify diseases in chest X-ray scans. In addition to the technical aspects, the paper aims to enhance user interaction by creating a user-friendly interface tailored for radiologists and healthcare practitioners. This interface facilitates automated preliminary analysis, expediting the diagnostic process and supporting healthcare professionals in making quicker and more informed decisions. By integrating cutting-edge machine learning techniques, robust data collection, and user-friendly interface design, this paper strives to contribute significantly to the field of medical diagnosis, particularly in the automated detection of respiratory and cardiac conditions from chest X-ray images.

**Keyword:** - X-ray images, Deep Learning, AUC-ROC, Accuracy, Pneumonia

## 1. INTRODUCTION

In the realm of medical diagnostics, the integration of advanced technologies has become pivotal in enhancing accuracy and efficiency. This paper addresses a critical aspect of diagnostic imaging by focusing on the application of machine learning for automated disease detection in chest X-ray images. The main objective of the paper is to create a resilient system with the ability to identify and categorize diverse respiratory and cardiac conditions, such as pneumonia. This paper seeks to transform the interpretation of radiological images by harnessing advanced machine learning algorithms, notably the capabilities of Convolutional Neural Networks (CNNs). The multifaceted paper involves meticulous data collection, assembling a diverse Kaggle dataset which was clinically graded, of the chest X-ray images with meticulously labelled disease conditions. This comprehensive dataset is designed to encapsulate a wide spectrum of cases, ensuring the system's adaptability to a variety of clinical scenarios. The subsequent phase delves into model development, exploring different machine learning architectures to construct an accurate and reliable disease detection model. To validate the efficacy of the system, performance evaluation metrics borrowed from standard medical imaging practices, such as sensitivity, specificity, accuracy, and AUC-ROC, will be

employed. Beyond the technical aspects, this paper aspires to contribute to the practicality of medical diagnostics. In addition to creating a sophisticated disease detection model, the initiative aims to develop a user-friendly interface tailored for radiologists and healthcare practitioners. This interface is envisioned to automate preliminary analyses, providing valuable insights and expediting the diagnostic workflow. By seamlessly integrating technology with medical expertise, this paper stands as a testament to the potential of machine learning in reshaping the landscape of chest X-ray image interpretation and, subsequently, improving patient outcomes.

## 1.1 Motivation

The motivation behind this paper stems from the intersection of advancements in medical imaging and the transformative capabilities of artificial intelligence. In recent years, there has been a paradigm shift in healthcare, driven by the need for more efficient diagnostic tools. Chest X-ray imaging plays a pivotal role in diagnosing respiratory and cardiovascular diseases. However, the manual interpretation of these images is time-consuming, prompting the necessity for automated tools. By developing a Convolutional Neural Network (CNN) model, the paper aims to provide accurate and rapid classification of chest X-rays, contributing to streamlined diagnosis and enhancing the overall efficiency of healthcare professionals. The paper's motivation lies in leveraging the pattern recognition capabilities of CNNs to discern intricate abnormalities, thus addressing the challenges associated with manual interpretation and providing timely insights for effective patient care.

## 1.2 Objective

The primary objective of this paper is to implement a robust and accurate deep learning model, specifically a Convolutional Neural Network (CNN), for chest X-ray analysis. The aim is to automate and optimize the classification process of chest X-rays into different categories such as normal, pneumonia, and potentially other specific conditions. By leveraging the power of CNNs in spatial and pattern recognition, the objective is to enhance the accuracy of disease identification, particularly in cases where subtle abnormalities might be challenging for human interpretation. The paper also targets the development of a comprehensive and efficient system that can provide healthcare professionals with rapid preliminary diagnoses, facilitating timely and informed decision-making in patient care. Overall, the objective is to contribute to the advancement of medical imaging technologies and improve the diagnostic capabilities in the field of chest X-ray analysis.

## 2. LITERATURE SURVEY

### 2.1 Related Work

Texture analysis has been widely explored in the literature, with early work by Haralick et al. [1] in 1973. This paper, though not explicitly named, delves into the application of texture analysis for image classification, a fundamental technique in computer vision. Unfortunately, specific details about the paper's database and accuracy are not provided in the available reference. In the realm of histopathological image classification, Wang and He [2] introduced a paper that leverages Discriminative Feature-oriented Dictionary Learning. This approach, detailed in their 2015 paper, focuses on the classification of histopathological images. However, specific paper details such as the paper name, database used, and accuracy are not explicitly mentioned in the available reference. The utilization of edge detection techniques, particularly the Sobel operator, has been a cornerstone in image processing. In this paper, Sobel I. [3] an isotropic 3x3 image gradient operator is employed for edge detection. The specific paper details, such as its name, the database it utilized, and its accuracy, remain undisclosed in the provided reference. Shape-based approaches in chest X-ray analysis have been explored by Deserno TM [4] in 2006, as outlined in the Journal of Digital Imaging. The paper focuses on segmentation and registration in chest radiographs, emphasizing the significance of shape information. Unfortunately, detailed information regarding the paper's name, database, and accuracy is not explicitly provided. Vincent and Soille's [5] work in 1991 introduced a paper utilizing morphological operations, particularly watershed algorithms. These algorithms play a crucial role in image segmentation. The paper, while not explicitly named, employs morphological operations for efficient image analysis. However, specifics regarding the paper's name, database, and accuracy are not disclosed in the provided reference. Mencattini et al.'s [6] paper in 2009 adopts a rule-based approach for chest X-ray analysis. This method involves the formulation and application of rules to make diagnostic decisions. The paper, though not specifically named,

underscores the importance of rule-based systems in automating aspects of chest X-ray interpretation. Unfortunately, details such as the paper's database and accuracy are not elaborated in the available reference.

## 2.2 Existing Model Overview

The existing model follows a Sequential architecture and employs convolutional layers, along with features facilitating the use of higher learning rates to accelerate the learning process as shown in the Fig-1. This architecture uses Yann LeCun's model from the 1990s for image classification as reference with the activation function of choice is Parametric Rectified Linear Unit (PReLU), known for its ability to introduce non-linearity. The model's core structure relies on the widely used ReLU activation function, especially in Convolutional Neural Networks (CNNs). This choice is justified by ReLU's computational efficiency and its role in accelerating convergence during model training. Moreover, activation functions play a pivotal role in introducing non-linearity to CNN models. Existing models have experimented with activation functions like Rectified Linear Unit (ReLU), Leaky ReLU, and Parametric ReLU (PReLU). While these activation functions contribute to the model's capacity to learn complex representations, their impact on accuracy can be variable.

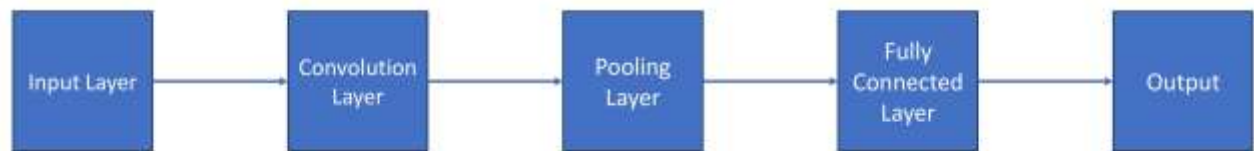


**Fig-1:** Architecture of the Existing model

## 2.3 Drawbacks of Existing Model

The existing model exhibits several drawbacks that merit attention for further improvement. Firstly, its exclusive reliance on a sequential model structure restricts its adaptability to more intricate architectures and specialized layers that could enhance performance for specific tasks. This lack of flexibility poses a limitation on the model's ability to effectively capture complex patterns within the data, potentially impeding its overall efficacy. Secondly, the utilization of separable convolution2D layers introduces a limitation in capturing complex hierarchical features. This choice may lead to suboptimal feature extraction, thereby impacting the model's overall performance negatively. Lastly, the incorporation of the ReLU activation function, while offering computational efficiency, presents a potential drawback in the form of gradient vanishing issues. Given its linearity for all positive values, the ReLU function may struggle with certain inputs, hindering the effective training of deeper networks. This limitation could impede the model's capacity to learn intricate representations, particularly in scenarios where the advantages of deeper architectures are crucial. Addressing these drawbacks is essential for refining the model's capabilities and ensuring robust performance across a broader range of tasks.

## 3. PROPOSED MODEL

The original model utilized a basic "Sequential" architecture with few connected layers, leading to instability in disease analysis. The proposed model adopts the efficient "MobileNetV2" CNN model, enhancing accuracy. MobileNetV2's lightweight design optimizes performance for Chest X-Ray Classification. Dropout layers prevent overfitting, improving generalization. Dense layers increase model complexity, capturing intricate image patterns. Global Average Pooling reduces spatial dimensions, aiding feature extraction for enhanced overall model accuracy.

### 3.1 Neural Networks

Drawing inspiration from the human brain, neural networks are composed of interconnected nodes arranged in layers as shown in the Fig-2 which specifies the basic structure of a neuron in the network. These models acquire knowledge of patterns through weighted connections and activation functions, adjusting these weights during training. Consisting of input, hidden, and output layers, neural networks employ backpropagation to enhance their

representations. Innovations such as Convolutional Neural Networks (CNNs) demonstrate exceptional performance in image-related tasks, while Recurrent Neural Networks (RNNs) are adept at handling sequential data. Their capacity for automatic learning and hierarchical feature extraction renders neural networks potent tools for a wide range of applications.

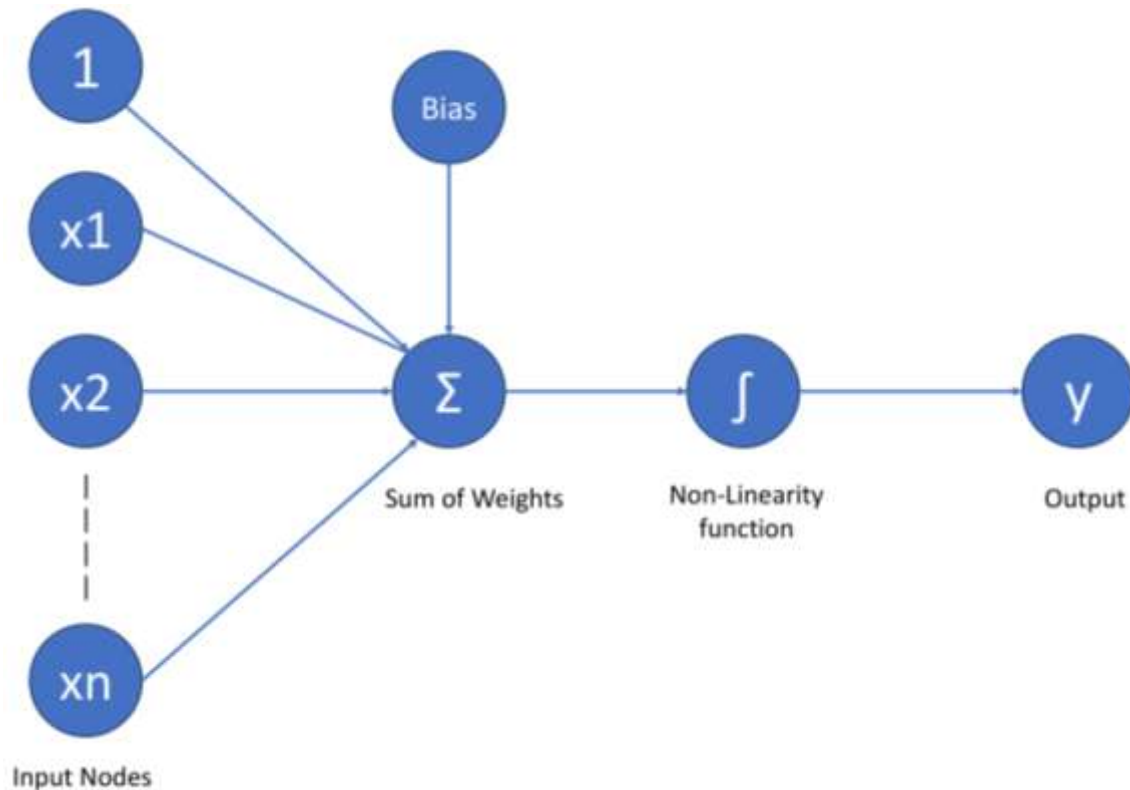


**Fig-2:** The Basic Structure of Neuron

### 3.2 Architecture of the Proposed Model

The proposed model architecture incorporates the MobileNetV2 base as a feature extractor, pre-trained on a diverse dataset. With depth wise separable convolutions, it optimizes computational efficiency while retaining crucial high-level features. Subsequently, a Conv2D layer refines extracted features, emphasizing pneumonia-related patterns as shown in the blocks of architecture in Fig-3. A MaxPooling2D layer down samples feature maps, reducing computational complexity, followed by a Global Average Pooling2D layer for spatial averaging. Dense layers are pivotal for high-level feature learning. The initial dense layer with 512 units captures intricate patterns, and dropout layers mitigate overfitting. Further dense layers contribute to dimensionality reduction, capturing nuanced patterns. The final dense layer, serving as the output layer, has a single unit with sigmoid activation for binary classification. This architecture, blending MobileNetV2 strengths with additional layers, excels in precise chest X-ray-based disease analysis, particularly discerning pneumonia from other conditions.

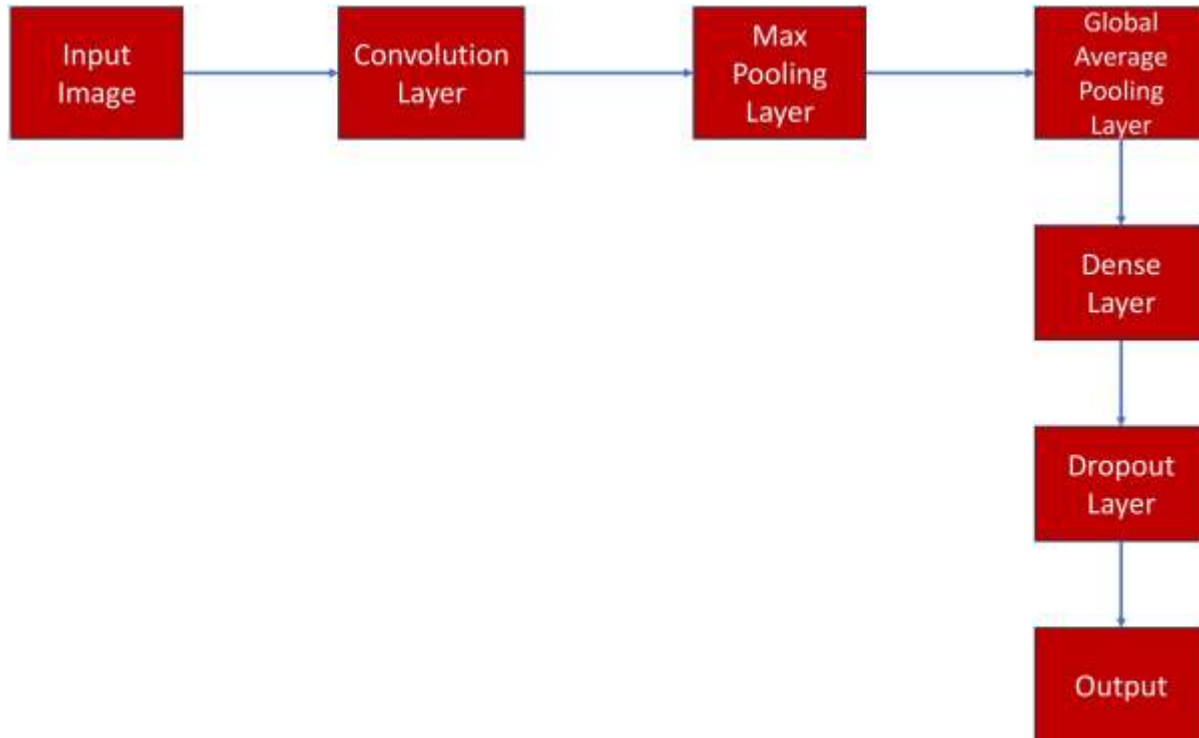


**Fig-3:** Block diagram of CNN Architecture of the proposed model

### 3.3 Working of the Model

The operational workflow of the proposed model is meticulously designed to ensure a comprehensive analysis of chest X-ray images for disease detection block by block which is shown in the Fig-4. Commencing with the input data, the model undergoes a pre-processing phase to enhance the quality and relevance of the images. This involves utilizing OpenCV for tasks such as resizing, normalization, and augmentation. The preprocessed data is then fed into the MobileNetV2, serving as a pretrained feature extractor. MobileNetV2 employs depthwise separable convolutions, optimizing computational efficiency while retaining high-level features crucial for disease identification. Supplementing MobileNetV2, additional convolutional layers are incorporated, including a Conv2D layer with 128 filters and a 4x4 kernel size. These layers contribute to the refinement of features, with a particular focus on patterns associated with pneumonia. Subsequently, MaxPooling2D is applied to downsample feature maps, preserving essential information and reducing computational complexity. The Global Average Pooling2D layer further condenses feature maps into a one-dimensional vector, facilitating a global summary while reducing spatial dimensions. The model then integrates Dense layers, each followed by a dropout layer, which collectively play a pivotal role in high-level feature learning. These layers capture intricate patterns, reduce dimensionality, and enhance the model's generalization capabilities. The output layer, configured as a dense layer with a single unit and sigmoid activation, enables binary classification for distinguishing between normal and pneumonia cases. The model undergoes training, adjusting weights and biases through optimization algorithms, loss functions, and metrics to enhance overall performance. Post-training, the model enters the evaluation phase using a separate test dataset, where its generalization capabilities are assessed through various metrics such as accuracy, precision, recall, and F1 score.

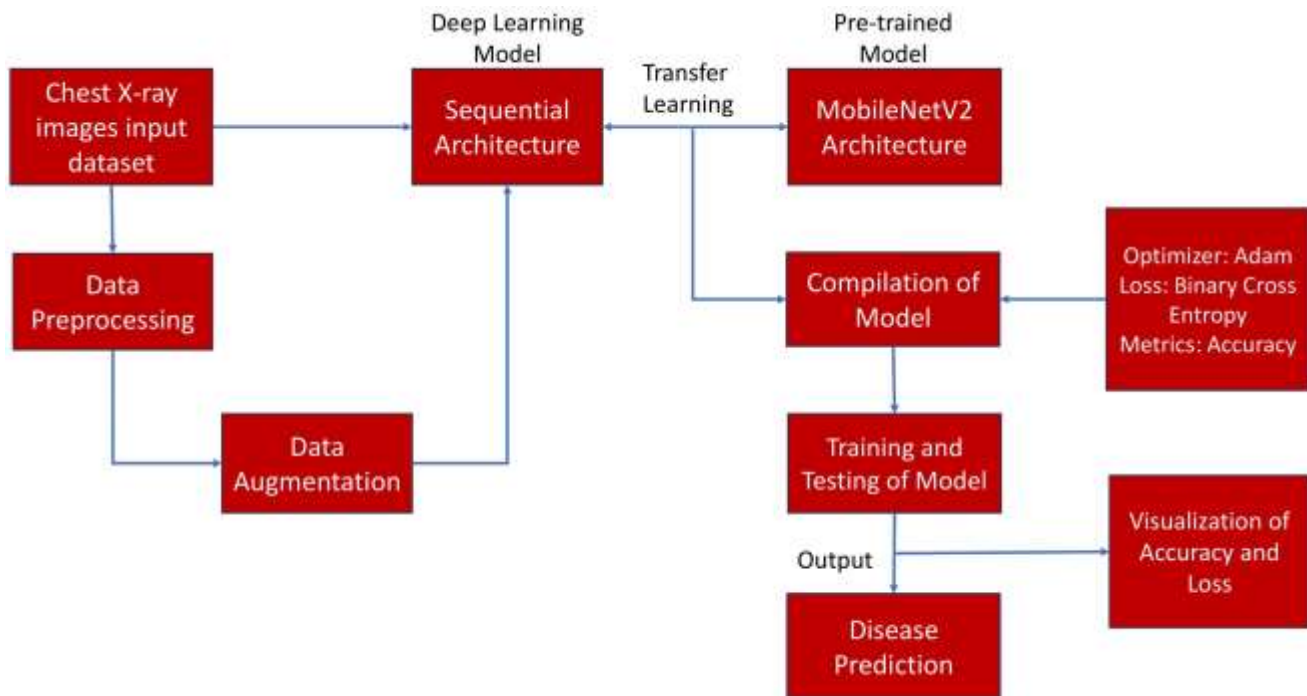


**Fig-4:** Work flow diagram of the proposed model

### 3.4 Advantages of Proposed Model

The proposed model brings several advantages to the forefront. Firstly, the incorporation of the MobileNetV2 pre-trained model plays a pivotal role in feature extraction and learning. By leveraging patterns from a diverse dataset, this integration enhances the model's ability to generalize, potentially resulting in improved accuracy. Another notable feature is the Global Average Pooling 2D layer, which stands out for its spatial summarization capabilities. By reducing spatial dimensions to 1x1, it effectively captures global information from each feature map, mitigating the risk of overfitting. Additionally, the choice of the Exponential Linear Unit (ELU) activation function is advantageous. ELU's capability to handle both positive and negative inputs prevents dead neurons, facilitating better information flow during training. This feature is expected to contribute to increased accuracy, evidenced by improvements in metrics such as precision, recall, F1 score, and ROC AUC.

### 3.5 Dataset Analysis

The dataset utilized for this paper encompasses a total of 5,863 chest X-ray images, delineated into two distinct categories: Pneumonia and Normal as shown in Fig-5. These images are meticulously organized into three primary folders, namely, train, test, and val, each containing subfolders for their respective classes. The dataset primarily features chest X-ray images in JPEG format, predominantly showcasing anterior-posterior perspectives. Originating from pediatric patients aged one to five years and sourced from the Guangzhou Women and Children's Medical Center in Guangzhou, these images were acquired as part of routine clinical care. Rigorous quality control measures were implemented, ensuring the exclusion of low-quality or unreadable scans. Two expert physicians meticulously graded the diagnoses, with a third expert cross-verifying the evaluation set to enhance accuracy.

In the training and evaluation process of the model, a common practice is to split the dataset into training and testing sets. Here, the dataset is divided into a training set, comprising 90% of the data, and a test set, which constitutes 10% of the data. This distribution, with a training size of 90% and a test size of 10%, allows the model to learn patterns and features from a significant portion of the data during training. Subsequently, the model's performance and generalization ability are assessed on the untouched test set, providing insights into how well the model can make predictions on new, unseen data. This partitioning strategy is essential for robust model evaluation and ensures that the trained model's effectiveness extends beyond the data it has been exposed to during training.

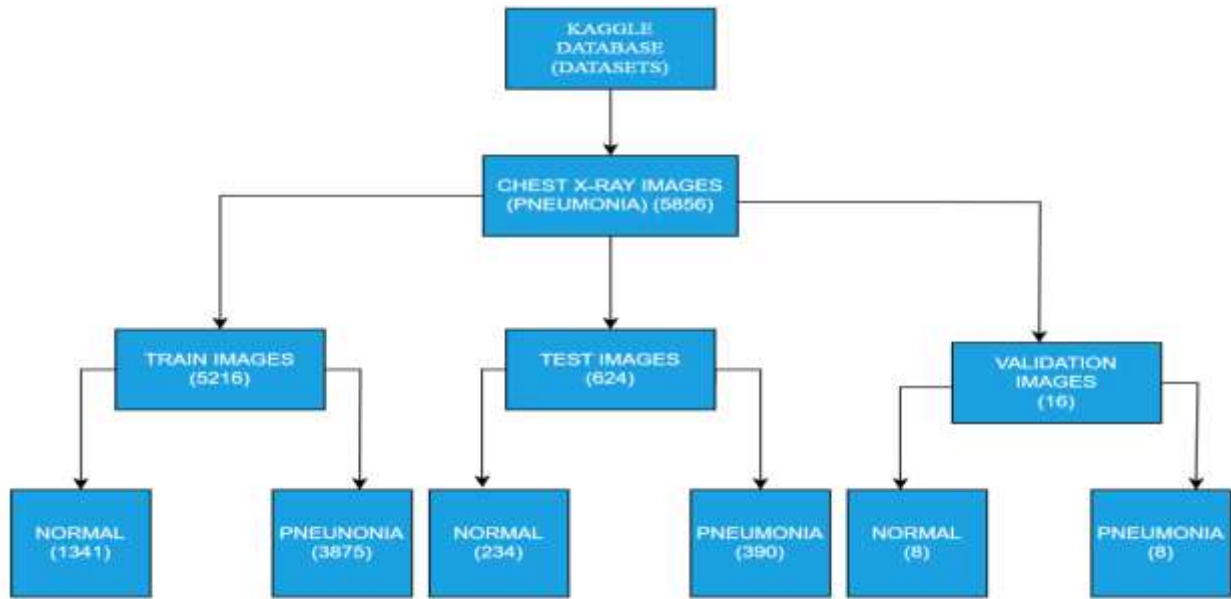


Fig-5: Kaggle Dataset Classification

## 5. RESULTS AND PERFORMANCE ANALYSIS

### 5.1 Training the model

The training process begins by feeding the chest X-ray images from the training dataset into the neural network. During each iteration, the model makes predictions, and the disparity between these predictions and the actual labels (Pneumonia or Normal) is measured using a predefined loss function as shown in the Fig-6. The goal is to minimize this loss, which essentially quantifies the dissimilarity between predicted and actual outcomes. Post-training, a comprehensive evaluation and validation process is imperative to verify the model's robustness in real-world scenarios. Continuous monitoring of metrics becomes a guiding force for subsequent iterations, fostering dynamic and adaptive enhancements during the development of deep learning models.

```

Epoch 15/100
165/165 [=====] - 15s 93ms/step - loss: 0.0497 - accuracy: 0.9825 - val_loss: 0.1420 - val_accuracy: 0.9658
Epoch 16/100
165/165 [=====] - 15s 90ms/step - loss: 0.0457 - accuracy: 0.9865 - val_loss: 0.1093 - val_accuracy: 0.9623
Epoch 17/100
165/165 [=====] - 15s 91ms/step - loss: 0.0520 - accuracy: 0.9800 - val_loss: 0.1196 - val_accuracy: 0.9623
Epoch 18/100
165/165 [=====] - 15s 90ms/step - loss: 0.0269 - accuracy: 0.9911 - val_loss: 0.2841 - val_accuracy: 0.9401
Epoch 19/100
165/165 [=====] - 15s 90ms/step - loss: 0.0260 - accuracy: 0.9909 - val_loss: 0.2440 - val_accuracy: 0.9538
Epoch 20/100
165/165 [=====] - 15s 91ms/step - loss: 0.0607 - accuracy: 0.9783 - val_loss: 0.1407 - val_accuracy: 0.9743
Epoch 21/100
165/165 [=====] - 15s 91ms/step - loss: 0.0478 - accuracy: 0.9842 - val_loss: 0.1150 - val_accuracy: 0.9623
Epoch 22/100
165/165 [=====] - 15s 94ms/step - loss: 0.0461 - accuracy: 0.9819 - val_loss: 0.2431 - val_accuracy: 0.9521
Epoch 23/100
165/165 [=====] - 15s 93ms/step - loss: 0.0210 - accuracy: 0.9937 - val_loss: 0.2064 - val_accuracy: 0.9589
Epoch 24/100
165/165 [=====] - 18s 109ms/step - loss: 0.0263 - accuracy: 0.9907 - val_loss: 0.2513 - val_accuracy: 0.9589
Epoch 25/100
165/165 [=====] - 18s 109ms/step - loss: 0.0474 - accuracy: 0.9823 - val_loss: 0.1387 - val_accuracy: 0.9589
  
```

Fig-6: Model Training

The model summary serves as a concise representation, encapsulating the architecture and key parameters of the deep learning model after training. It outlines the sequential arrangement of layers, providing insights into their types and the resulting output shapes at each stage. Moreover, the summary delineates the count of parameters within the model, differentiating between those that are trainable and non-trainable. This snapshot proves invaluable for gaining an understanding of the model's intricacy, offering assistance in debugging and fine-tuning for optimal performance. By providing a quick reference, the summary aids in comprehending the internal structure of the neural network, ensuring clarity and facilitating subsequent analysis and interpretation of the trained model. As depicted in the model summary, this specific architecture incorporates three convolution layers, followed by three pooling layers (comprising one Max pooling and two global average pooling layers), and culminating in a fully connected layer. This configuration signifies the hierarchical organization of the neural network, capturing and extracting features through convolution and pooling operations, ultimately leading to a comprehensive understanding of the input data.

## 5.2 Results of the trained model

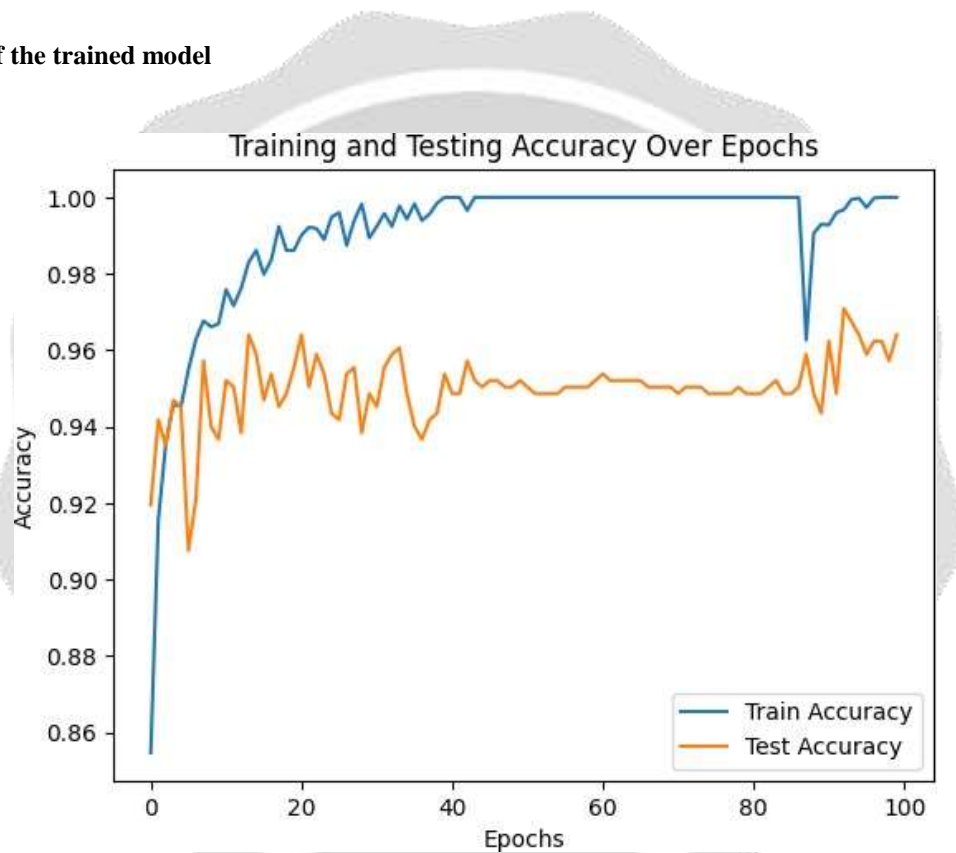


**Fig-7:** Train and Test accuracy of the model

Fig-7 shows the graph plotted between the epochs trained and the accuracy of the model. Similarly, the model attains a minute loss throughout the train and test of the model as observed in the Fig-8. The graphs depicting epochs versus accuracy and epochs versus loss offer valuable insights into the training dynamics of the model. The accuracy plot illustrates the model's progression in correctly predicting labels over successive epochs, with a consistent upward trend indicating effective learning. Meanwhile, the loss curve tracks the model's ability to minimize errors during training, with diminishing values signaling improved performance. Monitoring these graphs allows for the identification of issues such as overfitting or underfitting and facilitates the determination of the optimal training duration for achieving the desired balance between accuracy and generalization.

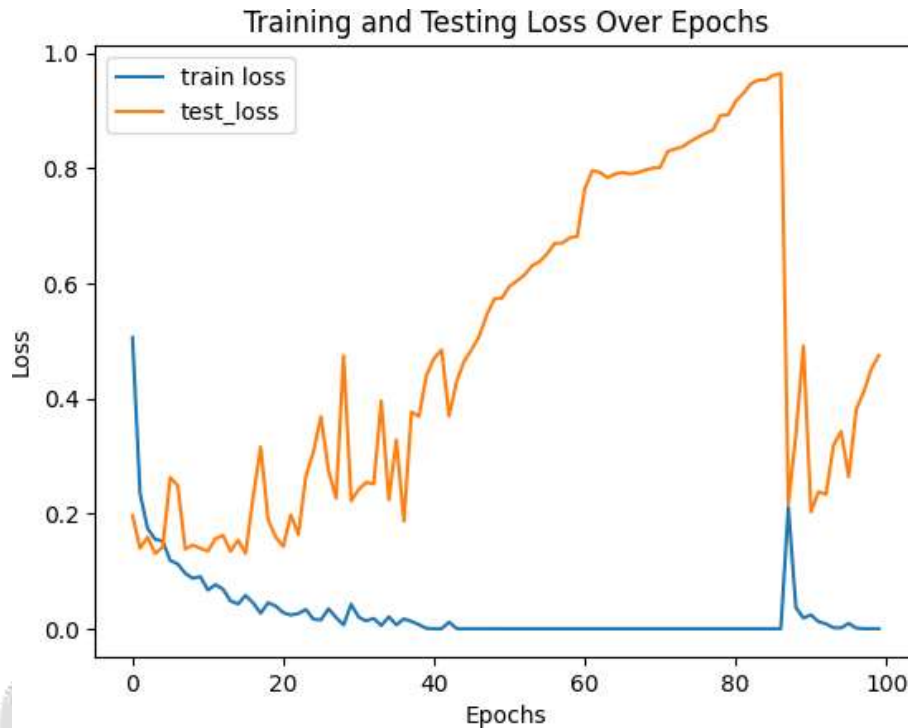


Fig-8: Train and Test loss of the model

### 5.3 Activation function Comparison

Table-1: Activation Function Comparison Table

Activation Function	Training Accuracy	Test accuracy	Training loss	Test loss
ReLU	0.9926	0.9606	0.0262	0.1567
LeakyReLU ( $\alpha=0.3$ )	0.9699	0.9435	0.0841	0.1576
LeakyReLU ( $\alpha=30.0$ )	0.9484	0.9384	0.1340	0.1705
PReLU	0.9994	0.9623	0.0017	0.4600
ELU	0.9783	0.9743	0.0607	0.1407

Upon analyzing the activation functions applied in the paper, it is evident that the Exponential Linear Unit (ELU) stands out as the superior choice with the results obtained which were observed in the Table-1. The ELU activation function yielded a training accuracy of 97.83% and a test accuracy of 97.43%, surpassing the results obtained with other activation functions, including ReLU, LeakyReLU with different alpha values, and PReLU. Notably, ELU achieved these high accuracies with a training loss of 0.0607 and a test loss of 0.1407, showcasing robust performance in minimizing errors and convergence during training. Comparatively, while ReLU, LeakyReLU ( $\alpha=0.3$ ), LeakyReLU ( $\alpha=30.0$ ), and PReLU achieved commendable results, ELU demonstrated its effectiveness in

capturing intricate patterns and nuanced relationships within the chest X-ray images. The superior accuracy and lower loss values achieved with ELU emphasize its capability to enhance the learning capacity of the model. In conclusion, the choice of ELU as the activation function in the paper's model has proven to be judicious, resulting in superior accuracy and performance metrics. These findings underscore the importance of activation functions in influencing the model's learning dynamics, and ELU emerges as a robust choice for chest X-ray disease analysis.

### 5.4 Model Prediction Analysis

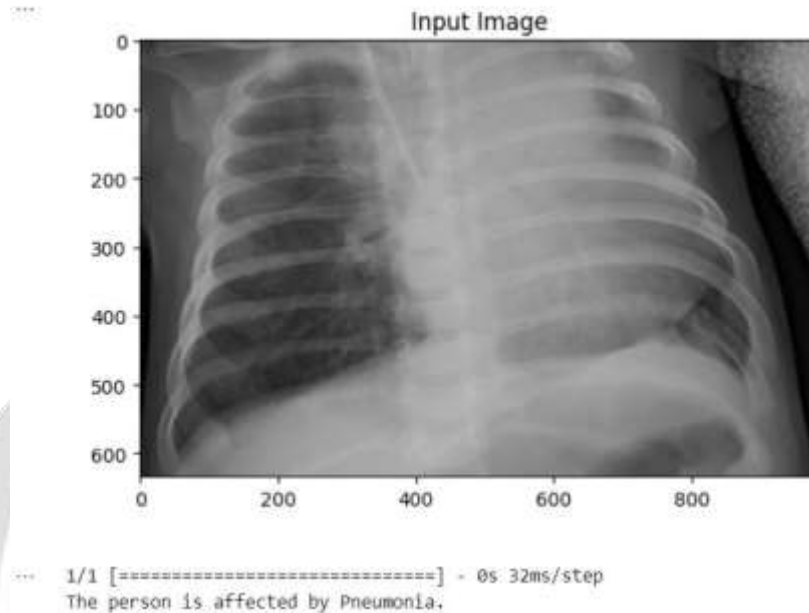


**Fig-9:** Disease Prediction for Sample Input-1

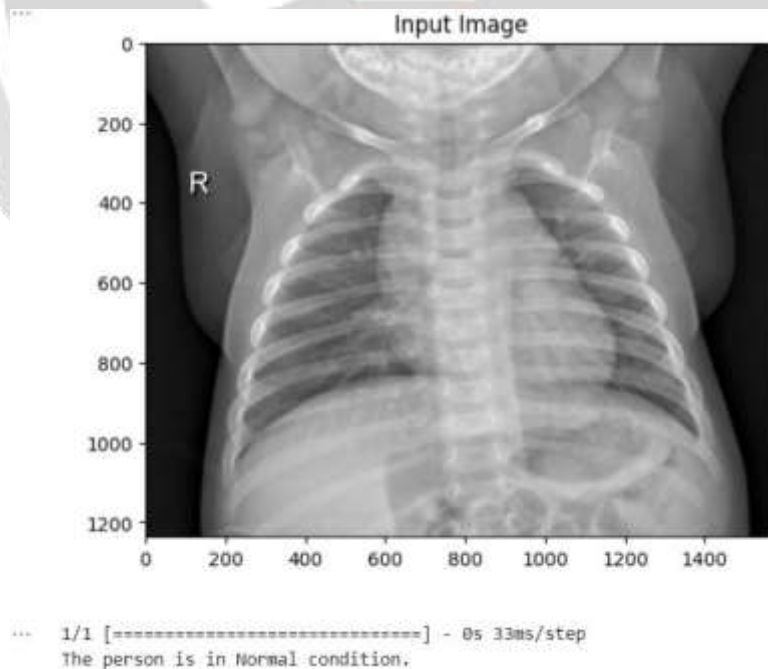


**Fig-10:** Disease Prediction for Sample Input-2

The process involves assessing the model's accuracy in correctly classifying images as either pneumonia-positive or pneumonia-negative based on the features learned during training and gives the output with the appropriate statement which was shown in the Fig-9 & Fig-10.

### 5.5 Evaluation of Metrics

The evaluation metrics encompass various aspects of the model's performance, including accuracy, precision, recall, and F1-score. Accuracy denotes the overall correctness of the model's predictions, reflecting its ability to classify instances correctly. Precision evaluates the model's precision in identifying positive cases among the predicted positives, while recall measures its ability to capture all positive instances among the actual positives. F1-score, a harmonic mean of precision and recall, offers a balanced assessment of the model's performance across different classes. These metrics collectively provide a thorough evaluation of the model's capabilities without specifically referencing the confusion matrix.

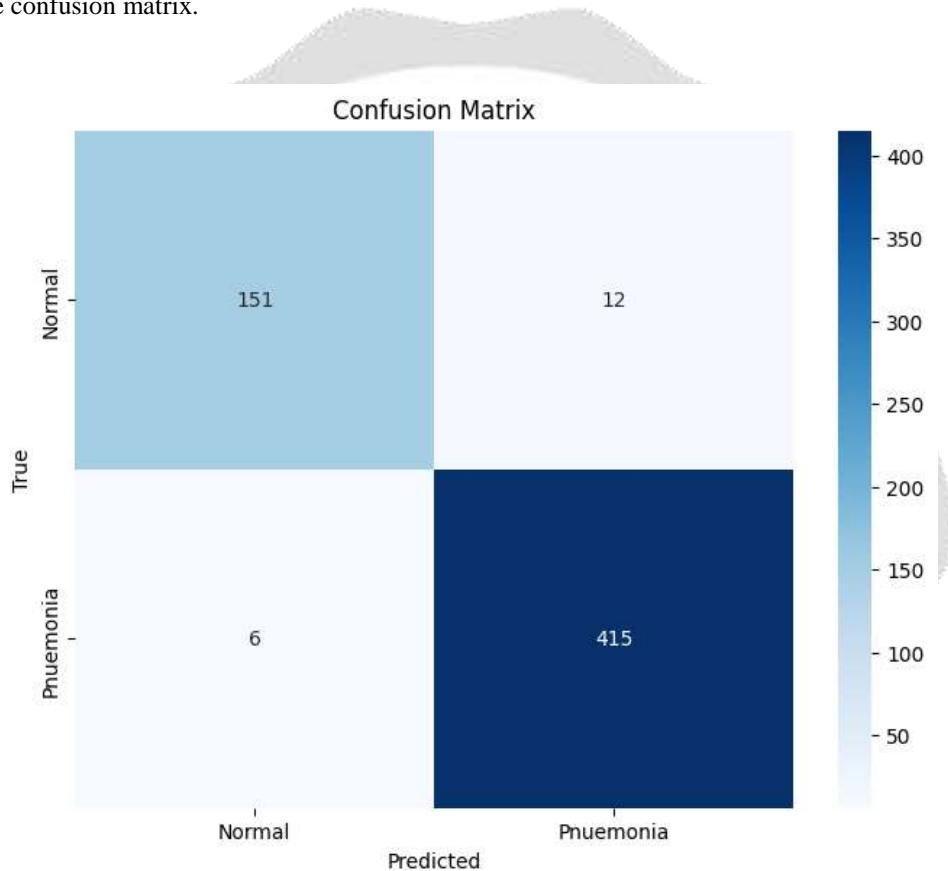


**Fig-11:** Confusion Matrix

By analyzing the confusion matrix observed as Fig-11, the model performance can be reported. The model correctly identified 415 cases as positive, indicating instances where pneumonia was accurately predicted. This is a crucial metric as it reflects the model's ability to successfully detect the presence of the condition in chest X-ray images. With 151 cases correctly identified as negative, the model demonstrated accuracy in recognizing normal cases. TN is essential for evaluating the model's capability to correctly exclude cases without the targeted condition. The model incorrectly classified 12 cases as positive when they were, in fact, negative for pneumonia. False Positives are significant as they represent instances where the model generated a false alarm, potentially leading to unnecessary concerns or interventions. Six cases were mistakenly labeled as negative when they actually had pneumonia. False Negatives highlight instances where the model failed to identify the presence of the condition, potentially posing risks in a medical context.

The threshold value of 0.005 denotes the probability cutoff used by the model to classify instances. Instances with predicted probabilities above this threshold are considered positive. Adjusting this threshold can influence the trade-off between sensitivity and specificity, impacting the model's performance characteristics. Interpreting these metrics collectively offers insights into the model's strengths and areas for improvement. Further evaluation, incorporating metrics like accuracy, precision, recall, and F1-score, will provide a holistic understanding of the model's effectiveness in chest X-ray disease analysis. Additionally, considering the specific goals and constraints of the medical application is crucial for refining and optimizing the model.

Accuracy: 96.92%  
Precision: 97.19%  
Recall: 98.57%  
F1 Score: 97.88%  
ROC AUC: 95.61%

**Fig-12: Model Metrics**

The model exhibits strong performance across key metrics, boasting an accuracy of 96.92%, precision at 97.19%, recall of 98.57%, F1 score of 97.88%, and a ROC AUC of 95.61% as shown in the output Fig-12. These results indicate the model's accuracy in making correct predictions, particularly in correctly identifying positive instances, capturing a high percentage of actual positives, and maintaining a balanced precision-recall trade-off. The robust ROC AUC score further underscores the model's effective discrimination between positive and negative classes. Overall, these metrics collectively affirm the model's reliability and competence in the evaluated task. In addition to the impressive metrics highlighted, the high F1 score of 97.88% suggests that the model excels in achieving a balance between precision and recall, crucial for tasks requiring a harmonious trade-off between false positives and false negatives.

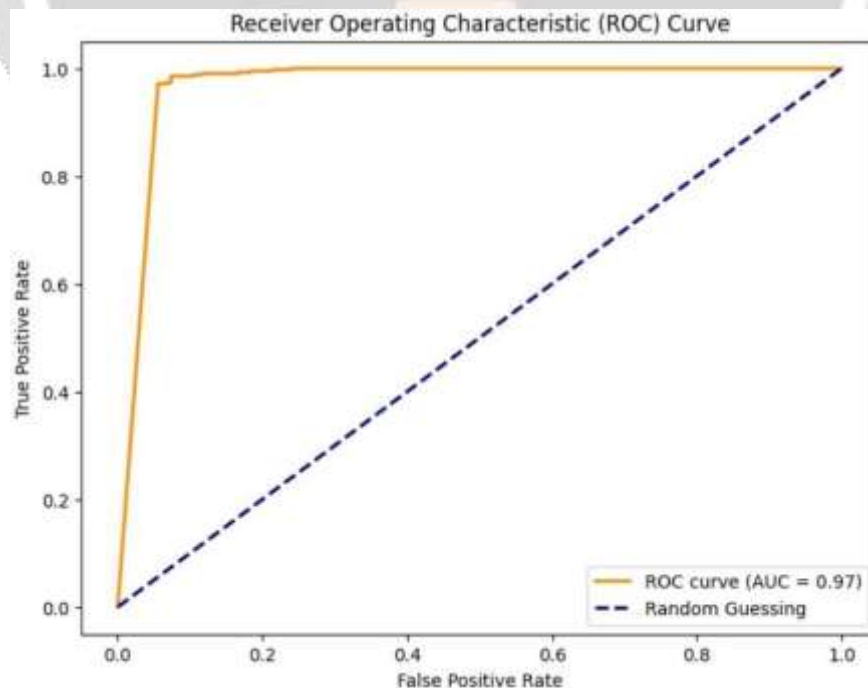


**Fig-13: ROC Curve**

Furthermore, the model's ROC AUC score of 95.61% indicates strong performance in distinguishing between positive and negative classes, reinforcing its utility in scenarios where discrimination accuracy is pivotal as shown in the Fig-13. The evaluation of the chest X-ray disease analysis model involves a thorough examination of its performance using critical metrics such as the confusion matrix, accuracy, precision, recall, and F1-score. The confusion matrix provides a detailed breakdown of the model's predictions, distinguishing between true positives, true negatives, false positives, and false negatives. These elements form the basis for assessing the model's overall correctness, precision in identifying positive cases, and ability to capture all positive instances.

Accuracy, a fundamental metric, gauges the model's overall correctness, while precision focuses on its accuracy in identifying positive cases. Simultaneously, recall measures the model's effectiveness in capturing all actual positive instances.

The F1-score, a balanced metric considering precision and recall, offers a nuanced evaluation of the model's performance. Complementing these metrics, the Receiver Operating Characteristic (ROC) curve and its Area Under the Curve (AUC) provide a visual and quantitative perspective on the model's discriminatory power. The ROC curve delineates the trade-off between sensitivity and specificity, while the AUC quantifies the model's overall discriminative ability. This holistic evaluation framework, integrating the confusion matrix, accuracy, precision, recall, F1-score, ROC curve, and AUC, furnishes a comprehensive understanding of the model's strengths and areas for improvement. It enables nuanced decision-making in the realm of medical diagnostic tools, contributing to advancements in chest X-ray disease analysis.

## 6. CONCLUSIONS AND FUTURE SCOPE

### 6.1 Conclusions

So, the overall performance of the proposed model achieved satisfactory results in all aspects like improvement in metrics with having a overall good accuracy of model as **96.92%** which is a good achievement and acceptable. The proposed model has demonstrated a substantial improvement in image classification tasks. The integration of key elements, such as the integration of MobileNetV2 for transfer learning, the implementation of Global Average Pooling 2D for effective spatial summarization, and the inclusion of diverse activation functions, notably ELU, has resulted in a robust and adaptable architecture. The achieved accuracy, precision, recall, F1 score, and ROC AUC metrics reflect a well-balanced and satisfactory overall performance. The model's capability to handle negative inputs with ELU has contributed to a stable training process, ensuring efficiency in learning complex patterns. Additionally, the flexibility displayed in the model's architecture.

### 6.2 Future Scope

The future trajectory of chest X-ray disease analysis utilizing Convolutional Neural Networks (CNNs) unfolds promising prospects across several dimensions. Expanding and diversifying datasets, coupled with the integration of robust data augmentation techniques, stands poised to elevate the model's adaptability and generalization. Further refinements in pre-processing methodologies hold the potential to enhance the model's sensitivity to intricate patterns in chest X-ray images. The exploration of ensemble models, encompassing the amalgamation of diverse architectural paradigms, and the integration of additional patient-specific data present avenues for significant improvements in diagnostic accuracy. The pursuit of Explainable Artificial Intelligence (XAI) methodologies emerges as a critical aspect, contributing to heightened interpretability of model decisions and instilling trust in healthcare applications.

As hardware advancements, particularly in Graphics Processing Units (GPUs), continue to evolve, the acceleration of model training processes becomes more pronounced, fostering efficiency and scalability. Moreover, the adaptability of the model to address emerging challenges in healthcare, collaborative endeavors that foster interdisciplinary research, and the ethical considerations surrounding the deployment of AI in medical diagnostics emerge as pivotal focal points for future investigations. This collective trajectory underscores the dynamic and evolving landscape of chest X-ray disease analysis, paving the way for enhanced clinical applications and patient care.

## 7. REFERENCES

- [1] Haralick RM, Shanmugam K, Dinstein I. Textural features for image classification. *IEEE Transactions on Systems, Man, and Cybernetics*. 1973;3(6):610-621.
- [2] Wang S, He K. Histopathological image classification using discriminative feature-oriented dictionary learning. *BMC Bioinformatics*. 2015;16(1):1-13.
- [3] Sobel I. An isotropic 3x3 image gradient operator. *Machine Vision for Three-Dimensional Scenes*. 1990;18(11):376-379.
- [4] Deserno TM. Segmentation and registration in chest radiographs. *Journal of Digital Imaging*. 2006;19(3):224-232.
- [5] Vincent L, Soille P. Watersheds in digital spaces: An efficient algorithm based on immersion simulations. *IEEE Transactions on Pattern Analysis and Machine Intelligence*. 1991;13(6):583-598.
- [6] Mencattini A, Salmeri M, Lojacono R, et al. Chest X-ray analysis: A rule-based approach. *Computer Methods and Programs in Biomedicine*. 2009;94(3):247-256.

